Tuning the ion selectivity of glutamate transporter–associated uncoupled conductances

Rosemary J. Cater, Robert J. Vandenberg, and Renae M. Ryan

Discipline of Pharmacology, Sydney Medical School, University of Sydney, Sydney, NSW 2006, Australia

The concentration of glutamate within a glutamatergic synapse is tightly regulated by excitatory amino acid transporters (EAATs). In addition to their primary role in clearing extracellular glutamate, the EAATs also possess a thermodynamically uncoupled Cl^- conductance. This conductance is activated by the binding of substrate and Na^+, but the direction of Cl^- flux is independent of the rate or direction of substrate transport; thus, the two processes are thermodynamically uncoupled. A recent molecular dynamics study of the archaeal EAAT homologue Glt_{Ph} (an aspartate transporter from *Pyrococcus horikoshii*) identified an aqueous pore at the interface of the transport and trimerization domains, through which anions could permeate, and it was suggested that an arginine residue at the most restricted part of this pathway might play a role in determining anion selectivity. In this study, we mutate this arginine to a histidine in the human glutamate transporter EAAT1 and investigate the role of the protonation state of this residue on anion selectivity and transporter function. Our results demonstrate that a positive charge at this position is crucial for determining anion versus cation selectivity of the uncoupled conductance of EAAT1. In addition, because the nature of this residue influences the turnover rate of EAAT1, we reveal an intrinsic link between the elevator movement of the transport domain and the Cl^- channel.

The Journal of General Physiology

INTRODUCTION

Glutamate is the predominant excitatory neurotransmitter in the central nervous system and is important in development, learning, memory, and higher cognitive function. Prolonged high synaptic glutamate concentrations are neurotoxic and thus need to be strictly regulated to prevent glutamate-mediated excitotoxicity (Vandenberg and Ryan, 2013). This regulation is maintained by the excitatory amino acid transporters (EAATs). Glutamate and aspartate transport via the EAATs is coupled to the cotransport of three Na^+ ions and one H^+ ion into the cell, and the counter-transport of one K^+ ion out of the cell (Zerangue and Kavanaugh, 1996; Levy et al., 1998; Owe et al., 2006).

Several crystal structures of an archaeal EAAT homologue, Glt_{Ph}, an aspartate transporter from *Pyrococcus horikoshii*, at different stages of the transport cycle have been solved (Yernool et al., 2004; Boudker et al., 2007; Reyes et al., 2009; Verdon and Boudker, 2012). Glt_{Ph} is a trimer where three identical protomers come together to form a bowl-like structure that sits within the cell membrane. Within this trimer, each protomer transports substrate and supports a Cl^- conductance independently (Grewer et al., 2005; Koch et al., 2007; Leary et al., 2007; Ryan and Mindell, 2007; Ryan et al., 2009). These protomers are wedge-like in shape, consisting of eight α-helical transmembrane domains (TM1–8) and two helical hairpin loops (HP1 and 2). Each protomer consists of two functional domains: the trimerization domain (consisting of TM1, TM2, TM4, and TM5), which is responsible for maintaining interactions between protomers, and the transport domain (consisting of TM3, TM6, HP1, TM7, HP2, and TM8), which contains the binding sites for aspartate and two of the three coupled Na^+ ions (Fig. 1 A). The structures of Glt_{Ph} in several different conformations have revealed that substrate transport via Glt_{Ph}, and by inference also the EAATs, is achieved through a large inward movement of the transport domain relative to the trimerization domain toward the cytoplasm (Reyes et al., 2009). This large inward movement is referred to as the elevator mechanism and has also been observed using single molecule fluorescence resonance energy transfer (Akyuz et al., 2015; Ryan and Vandenberg, 2016).

In addition to transporting glutamate, the EAATs also possess Cl^- channel activity, which is known to have a physiological role in ionic and osmotic balance (Vandenberg et al., 2008, 2011). In the retina, activation of the Cl^- channel function of EAAT5 results in hyperpolarization of neurons and contributes to a negative feedback loop that leads to a reduction in glutamate release and excitatory transmission (Veruki et al., 2006). This Cl^- channel is activated by the binding of substrate and Na^+, but the direction of Cl^- flux is independent of the rate or direction of substrate transport, and thus the two processes are thermodynamically uncoupled (Fair-

Correspondence to Renae M. Ryan: renae.ryan@sydney.edu.au

Abbreviations used in this paper: EAAT, excitatory amino acid transporter; TBOA, DL-threo-β-benzyloxyaspartate.

© 2016 Cater et al. This article is distributed under the terms of an Attribution–Noncommercial–Share Alike–No Mirror Sites license for the first six months after the publication date (see http://www.rupress.org/terms). After six months it is available under a Creative Commons License (Attribution–Noncommercial–Share Alike 3.0 Unported license, as described at http://creativecommons.org/licenses/by-nc-sa/3.0/).

The Rockefeller University Press $30.00
J. Gen. Physiol. 2016 Vol. 148 No. 1 13–24
www.jgp.org/cgi/doi/10.1085/jgp.201511556

CrossMark

Downloaded from http://rupress.org/jgp/article-pdf/148/1/13/1795669/jgp_201511556.pdf by guest on 05 December 2025

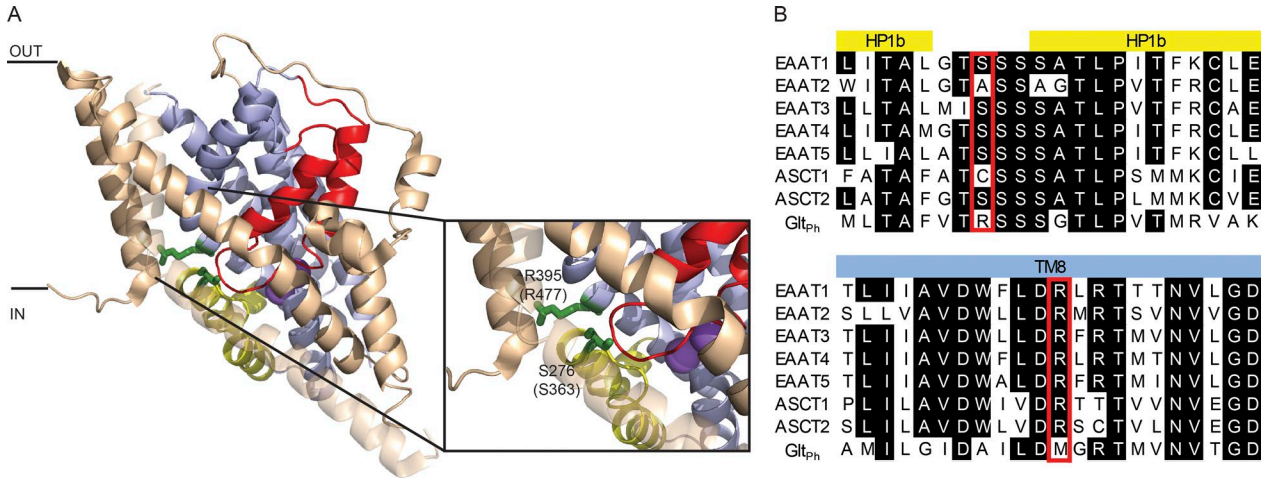

Figure 1. **Structural conservation of an arginine residue at the interface of the transport domain and trimerization domain.** (A) Cartoon representation of a locked R276S/M395R Glt_{Ph} protomer in the plane of the membrane in the outward-facing occluded state (PDB accession no. 4X2S). The trimerization domain (TM1, TM2, TM4, and TM5) is colored in light brown, and the transport domain (TM3, TM6, TM7, TM8, HP1, and HP2) is colored in light blue, with HP1 and HP2 highlighted in yellow and red, respectively. In this mutant Glt_{Ph} structure, the arginine has been moved from the native position of 276 to 395 to reflect the position of this positively charged residue in the EAATs. Residues 276 and 395 are shown in green stick representation and numbered according to Glt_{Ph} positioning, with EAAT1 numbering provided in parentheses. Na^+ ions are represented as purple spheres. Aspartate is not present in this structure. The figure was made using the software PyMOL (The PyMOL Molecular Graphics System, version 1.3r1; Schrödinger, LLC). (B) Amino acid alignment of HP1 and TM8 of the SLC1 family. R276/S363 and M395/R477 are outlined in red.

man et al., 1995; Wadiche et al., 1995). Estimations place the minimum pore diameter of this channel at ∼6 Å, which allows the permeation of a range of anions. These anions have a permeability sequence of $SCN^- > NO_3^- > I^- > Br^- > Cl^- >> F^-$, where SCN^- is the most permeant anion (Wadiche and Kavanaugh, 1998). It has been demonstrated through sulfhydryl modification of introduced cysteine residues in HP2 of EAAT1 and EAAT3 that the molecular determinants responsible for Cl^- conductance are distinct from those responsible for substrate transport (Seal et al., 2001; Borre et al., 2002; Ryan and Vandenberg, 2002). However, these molecular determinants cannot be observed in existing Glt_{Ph} crystal structures as these structures do not feature an open Cl^- channel.

Mutagenesis, structural, and molecular dynamics studies have located the EAAT1 anion conductance pathway at the interface of the transport and trimerization domains (referred to here as the domain interface), and it has been proposed that after the binding of substrate, this pathway transiently opens up as the transport domain moves toward the cytoplasm upon substrate transport (Ryan and Vandenberg, 2005; Ryan and Mindell, 2007; Vandenberg et al., 2008; Verdon and Boudker, 2012; Cater et al., 2014, 2016; Machtens et al., 2015; Torres-Salazar et al., 2015). A recent study by Machtens et al. (2015) proposed a Cl^--conducting conformation in Glt_{Ph} through the use of molecular dynamics. This conformation exists at an early intermediate stage of the transport cycle and involves a lateral movement of the transport domain relative to the trimerization domain. The proposed pathway is a predominantly hydrophobic hourglass-shaped pore at the domain interface. This pore is well hydrated and runs almost perpendicular to the membrane. In the middle of this hydrated hydrophobic pore lies a positively charged arginine residue (Arg-276) that protrudes from the tip of HP1 into the center of the proposed Cl^- channel. It has been suggested that this arginine residue confers anion selectivity through EAAT2–4 and Glt_{Ph}-uncoupled conductance pathways (Borre and Kanner, 2004; Machtens et al., 2015).

It is interesting to note that the location of this arginine residue differs between the secondary structures of the EAATs and Glt_{Ph} (TM8 and HP1, respectively), despite occupying a similar position in the tertiary structure of both transporters (Fig. 1). Here, we have mutated this arginine residue in EAAT1 to a histidine (R477H) and analyzed the pH dependence of substrate transport and uncoupled anion conductances using two-electrode voltage-clamp electrophysiology. Our results reveal that a positive charge at this position is necessary for selectivity of anions over cations through the EAAT1 anion channel and that the nature of this residue determines the turnover rate of EAAT1.

MATERIALS AND METHODS

Site-directed mutagenesis

EAAT1 cDNA was subcloned into the plasmid oocyte transcription vector (pOTV). Site-directed mutagenesis was performed using the Q5 site-directed mutagenesis

Downloaded from http://rupress.org/jgp/article-pdf/148/1/13/1795669/jgp_201511556.pdf by guest on 05 December 2025

kit (New England Biolabs, Inc. [Genesearch]) and oligonucleotide primers synthesized by Sigma-Aldrich. The sequences of cDNA products were confirmed by the Australian Genome Research Facility. WT EAAT1 and mutant cDNAs were linearized with Spe1 (New England Biolabs, Inc. [Genesearch]) and transcribed to cRNA by T7 RNA polymerase using the mMESSAGE mMACHINE kit (Ambion).

Harvesting and preparing oocytes

All chemicals were purchased from Sigma-Aldrich unless otherwise stated. *Xenopus laevis* frogs were obtained from NASCO. Stage V oocytes were harvested from *Xenopus* as previously described (Poulsen and Vandenberg, 2001), with all surgical procedures in accordance with the Australian Code of Practice for the Care and Use of Animals for Scientific Purposes. Defoliculated stage V oocytes were injected with 4.6 ng cRNA (Drummond Nanoject; Drummond Scientific Co.) and subsequently incubated at 16–18°C in standard frog Ringer's solution (ND96: 96 mM NaCl, 2 mM KCl, 1 mM $MgCl_2$, 1.8 mM $CaCl_2$, and 5 mM HEP ES, pH 7.5) supplemented with 50 µg/ml gentamycin, 2.5 mM sodium pyruvate, 50 µg/ml tetracycline, and 0.5 mM theophylline.

Electrophysiology

2–4 d after injections, currents were recorded using the two-electrode voltage-clamp technique with a GeneClamp 500 amplifier (Axon Instruments) interfaced with a PowerLab 2/20 chart recorder (ADInstruments) and a Digidata 1322A (Axon Instruments) used in conjunction with Chart software (ADInstruments; Axon Instruments). All recordings were made with a bath grounded via a 3 M KCl/agar bridge linking to a 3 M KCl reservoir. Unless otherwise stated, background currents were eliminated by subtracting currents in the absence of substrate from substrate-elicited currents at corresponding membrane potentials. The pH of extracellular buffers was adjusted using H_2SO_4 and Trizma base.

Substrate concentration responses were performed at pH 5.5, 6.5, 7.5, and 8.5. Current at −60 mV (I) was fit by least squares to a derivation of the Michaelis–Menten equation (Eq. 1):

$$I/I_{max} = [S]/(K_{0.5} + [S]), \quad (1)$$

where I_{max} is the maximal current, $[S]$ is the substrate concentration, and $K_{0.5}$ is the concentration of substrate required to produce the half maximal current.

Na^+ titrations were conducted at pH 5.5 for WT EAAT1 and R477H in the presence of 300 µM or 3 µM glutamate for WT EAAT1 and R477H, respectively. Choline$^+$ (Ch^+) was used to balance osmolarity and does not support substrate transport. The current at −60 mV (I) was fit by least squares to a derivation of the Hill equation (Eq. 2):

$$I/I_{max} = [Na^+]^h/(K_{0.5}{}^h + [Na^+]^h), \quad (2)$$

where I_{max} is the maximal current, $[Na^+]$ is the Na^+ concentration, h is the Hill slope, and $K_{0.5}$ is the concentration of Na^+ required to produce the half maximal current.

Current-voltage relationships for substrate-elicited conductances were determined by measuring substrate-elicited currents during 200-ms voltage pulses from −30 mV to membrane potentials ranging from −100 to 60 mV at 10-mV steps. To investigate the nature of uncoupled conductances through WT EAAT1 and R477H, submaximal glutamate-elicited current-voltage relationships were determined in ND96 and 96 mM gluconate buffer (96 mM Na^+ gluconate, 2 mM K^+ gluconate, 1 mM Mg^{2+} gluconate, 1.8 mM Ca^{2+} gluconate, and 5 mM HEPES) at pH 5.5, 6.5, 7.5, and 8.5. Additionally, the permeabilities of Cl^- and Na^+ through the uncoupled conductance pathways of WT EAAT1 and R477H at pH 5.5 and 8.5 were investigated by determining current-voltage relationships at a range of different Cl^- and Na^+ concentrations at these pH levels. Choline$^+$ and gluconate$^-$ were used as the substituted cation and anion, respectively, to obtain correct osmotic balance as they do not support substrate transport or permeate the transporter's uncoupled conductance pathway.

To investigate whether changes in $K_{0.5}$ for glutamate and aspartate at pH 5.5 were caused by changes in the substrate-binding site or changes in elevator movements of the transport domain, the nontransportable blocker DL-threo-β-benzyloxyaspartate (TBOA; Tocris Bioscience) was used. TBOA blocks the EAAT1 Na^+-activated anion conductance (Ryan et al., 2004), and therefore, we can measure the affinity of TBOA for the transporter in the absence of any competing substrate. Steady-state currents were measured in the presence of increasing concentrations of TBOA at 60 mV and were subtracted from currents in the absence of TBOA. These concentration response experiments were conducted for oocytes expressing either WT EAAT1 or R477H at pH 5.5 in 96 mM NO_3^- buffer (96 mM $NaNO_3$, 2 mM KNO_3, 1 mM $Mg(NO_3)_2$, 1.8 mM $Ca(NO_3)_2$, and 5 mM HEP ES) to amplify the magnitude of the Na^+-activated anion conductance. TBOA blockage of the Na^+-activated anion conductance at 60 mV (I) was fit by least squares to a derivation of the Michaelis–Menten equation (Eq. 1).

Relative anion permeabilities (P_X/P_{Cl}; X denoting Br^-, I^-, or NO_3^-) for WT EAAT1 and R477H were determined at pH 5.5 and 8.5 by measuring the reversal potentials (E_{rev}) of substrate-elicited conductances in recording solution containing 10 mM Na^+ salts of Cl^-, Br^-, I^-, or NO_3^- and 86 mM Na^+-gluconate (to obtain 96 mM Na^+), 2 mM K^+-gluconate, 1 mM Mg^{2+}-gluconate, 1.8 mM Ca^{2+}-gluconate, and 5 mM HEPES. 10 mM per-

Downloaded from http://rupress.org/jgp/article-pdf/148/1/13/1795669/jgp_201511556.pdf by guest on 05 December 2025

meant anion concentrations were used to minimize anion loading of oocytes that could otherwise affect reversal potential measurements. Reversal potential measurements (E_{rev}) were then substituted into the Goldman–Hodgkin–Katz equation (Eq. 3):

$$E_{rev} = (RT/zF)\ln(P_X[X^-]_{out}/P_{Cl}[Cl^-]_{in}), \quad (3)$$

with R being the gas constant, T temperature in degrees Kelvin, z the charge of the anion, and F Faraday's constant. We assumed $[Cl^-]_{in}$ = 41 mM (Barish, 1983) to calculate P_X/P_{Cl}.

Radiolabeled uptake

Uptake of L-[^{3}H]glutamate (PerkinElmer) into oocytes expressing WT EAAT1 and R477H was measured at pH 5.5, 6.5, 7.5, and 8.5. Oocytes expressing WT EAAT1 were incubated in 10 µM L-[^{3}H]glutamate, whereas those expressing R477H were incubated in ND96 containing 200 nM, 300 nM, 1 µM, and 10 µM L-[^{3}H]glutamate at pH 5.5, 6.5, 7.5, and 8.5, respectively, to account for pH-dependent shifts in the $K_{0.5}$ for glutamate. After specified incubation times, uptake was terminated by washing oocytes three times in ice-cold ND96. Oocytes were then lysed with 1 M NaOH + SDS (1% wt/vol). After the addition of scintillant (Ultima Gold; Packard), counting was performed using a MicroBeta TriLux scintillation counter (PerkinElmer).

Data analysis

Analysis of kinetic data was conducted using Prism software version 5.0 (GraphPad Software). All values presented refer to the mean of at least four oocytes from a minimum of two batches of oocytes.

RESULTS

The aim of this study was to investigate the role of an arginine residue (R477) in determining anion selectivity of the uncoupled conductance of the human glutamate transporter, EAAT1. Arg-477 is close to the substrate-binding site and is predicted to protrude into the uncoupled anion permeation pathway of EAAT1 (Fig. 1 A; Boudker et al., 2007; Machtens et al., 2015). We have mutated this arginine residue to a histidine (R477H) and manipulated the pH of the recording buffer to investigate the influence of the protonation state of this residue on substrate transport properties and anion selectivity of the uncoupled conductance.

pH dependence of substrate transport

Arg-477 is close to the substrate-binding site and protrudes into the interface between the transport and trimerization domains (Fig. 1 A). Therefore, mutagenesis of this residue may alter the nature of substrate recognition or alter the movement of the transport domain relative to the trimerization domain during the "elevator movement" required for translocation. L-Glutamate applied to oocytes expressing WT EAAT1 or R477H generates inward currents when cells are voltage clamped at −60 mV (Fig. 2, A–C). To examine the effects of the R477H mutation on glutamate transport, the half-saturation of glutamate- and aspartate-activated currents ($K_{0.5}$) for WT EAAT1 and the R477H mutant transporter were measured at pH values ranging from 5.5 to 8.5 in oocytes clamped at −60 mV. For WT EAAT1, pH had a slight effect on $K_{0.5}$ (Fig. 2 D and Table 1). In contrast, the R477H transporter demonstrated clear pH dependence for the $K_{0.5}$ of both glutamate and aspartate (Fig. 2 E and Table 1). At pH 5.5, the R477H mutant transporter has a $K_{0.5}$ for glutamate of 0.70 ± 0.03 µM, ∼45-fold lower than that of WT EAAT1 under the same conditions (32 ± 3 µM). With increasing extracellular pH, the glutamate $K_{0.5}$ for R477H increases to 64 ± 8 µM (∼100-fold higher than at pH 5.5), returning to a value more similar to that of WT EAAT1 at pH 8.5 (41 ± 2 µM; Fig. 2, D and E; Fig. 4 A; and Table 1). To establish whether the lower $K_{0.5}$ of the R477H mutant transporter at pH 5.5 was caused by changes in the Na^+ dependence of transport, Na^+ titrations were performed for WT EAAT1 and R477H at pH 5.5 (Fig. 2 F). These experiments revealed that the $K_{0.5}$ of Na^+ for WT EAAT1 and R477H were similar (50 ± 10 mM and 77 ± 8 mM), as was the Hill coefficient (1.5 ± 0.1 and 1.8 ± 0.1), supporting the notion that Na^+ coupling is not altered in the R477H mutant transporter.

Next, we measured L-[^{3}H]glutamate uptake by oocytes expressing WT EAAT1 and R477H transporters at pH values ranging from 5.5 to 8.5 over a 10-min period. For WT EAAT1, an increase in pH, i.e., a decrease in $[H^+]$, resulted in a subtle decrease in L-[^{3}H]glutamate uptake from 68 ± 2 pmol/oocyte at pH 5.5 to 50 ± 1 pmol/oocyte at pH 8.5 (Fig. 3 A). This is expected as a H^+ is cotransported into the cell with glutamate and decreasing extracellular $[H^+]$ will reduce the driving force for transport via EAAT1. In contrast, the R477H mutant transporter demonstrated a striking pH dependence for L-[^{3}H]glutamate uptake. At pH 5.5, uptake of L-[^{3}H]glutamate via R477H was 0.95 ± 0.03 pmol/oocyte. In a pH-dependent manner, the amount of L-[^{3}H]glutamate uptake by R477H increased to a level of 28.9 ± 0.6 pmol/oocyte at pH 8.5 (Fig. 3 B). Uptake at pH 8.5 for the R477H mutant transporter is comparable with that of WT EAAT1 and demonstrates that the expression of R477H is similar to WT EAAT1. The increased $K_{0.5}$ for glutamate and the low levels of glutamate uptake of R477H at pH 5.5 over 10 min suggest that under these conditions, the mutant transporter has a significantly slower turnover rate. To investigate this further, we performed glutamate uptake for WT EAAT1 and R477H at pH 5.5 and 8.5 over a 120-min time course (Fig. 3, C and D). These results reveal that the turnover rate of

Downloaded from http://rupress.org/jgp/article-pdf/148/1/13/1795669/jgp_201511556.pdf by guest on 05 December 2025

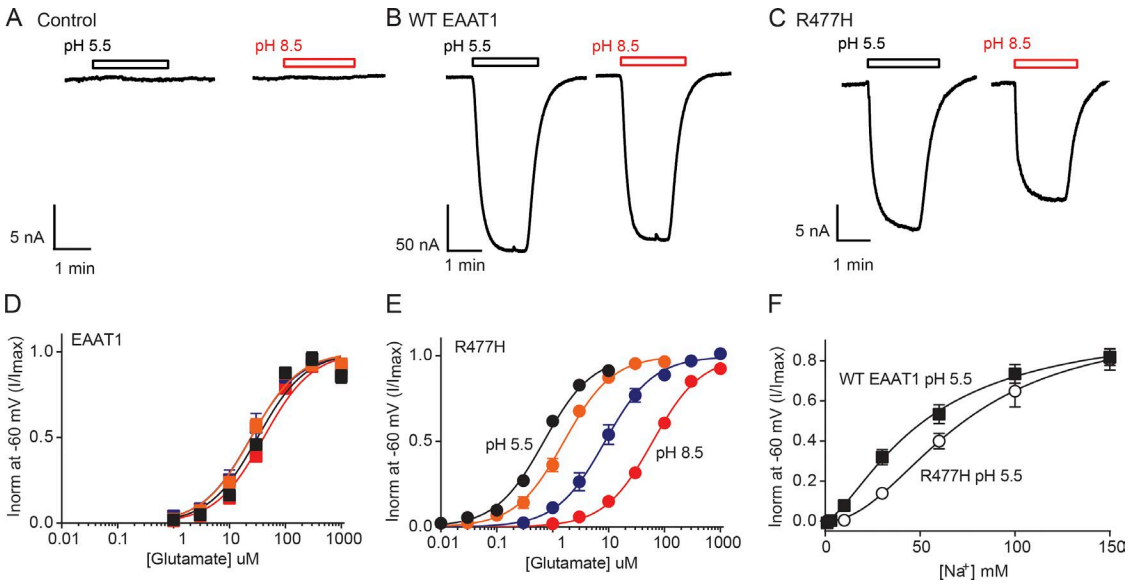

Figure 2. **R477H presents strong pH dependence for apparent glutamate affinity.** (A–C) Representative current traces elicited by $K_{0.5}$ concentrations (see Table 1) of L-glutamate for control (uninjected oocytes; A), WT EAAT (B), and R477H (C) at pH 5.5 (black bars) and 8.5 (red bars). (D and E) L-Glutamate concentration responses for WT EAAT1 (D) and R477H (E) were conducted at −60 mV in ND96 at pH 5.5 (black), 6.5 (orange), 7.5 (blue), and 8.5 (red). (F) Na^+ concentration responses were performed at −60 mV for WT EAAT1 (closed squares) and R477H (open circles) at pH 5.5 in the presence of 300 µM or 3 µM L-glutamate for WT EAAT1 or R477H, respectively. $Choline^+$ was used as the substitute cation. Currents were normalized to the maximal current activated for each cell. Data shown represent the mean ± SEM ($n \geq 3$). Where error bars cannot be seen, they lie within the symbol.

R477H at pH 5.5 (0.047 ± 0.001 pmol/oocyte/min) is reduced compared with WT EAAT1 (3.5 ± 0.4 pmol/oocyte/min) and R477H (1.4 ± 0.1 pmol/oocyte/min) at pH 8.5, but the mutant transporter can accumulate glutamate over background levels and is therefore a functional transporter.

The striking pH dependence of substrate transport properties demonstrated by the R477H mutant transporter seems counterintuitive considering that at pH 5.5 the majority of His-477 residues will be protonated and more closely resemble the charge of the native arginine residue found at this position in WT EAAT1. To investigate whether these changes were caused by a rearrangement of the substrate-binding site or a disruption to the elevator mechanism, which allows for the translocation of substrate to the cytoplasm (Reyes et al., 2009), we examined the ability of a nontransportable competitive inhibitor TBOA to bind to the substrate-binding site. The aspartate moiety of TBOA binds to the same site as aspartate, whereas the benzoyl moiety of TBOA prevents HP2 from closing and the subsequent translocation of the transport domain (Boudker et al., 2007). This effectively arrests the transporter in an outward-facing conformation. To measure the interaction of TBOA with the binding site, we applied increasing concentrations of TBOA to oocytes expressing WT EAAT1 and the R477H mutant at pH 5.5 as this is where we observe the largest difference in substrate $K_{0.5}$. The application of TBOA alone is known to block a leak conductance carried by Cl^- ions through the EAATs (Ryan et al., 2004), and we can measure an affinity of the interaction of TBOA with the transporter in the absence of any competing substrate. Interestingly, the $K_{0.5}$ of TBOA for both WT EAAT1 (2.6 ± 0.4 µM) and the R477H transporter (6.3 ± 0.4 µM) at pH 5.5 are comparable (Fig. 4 A) and cannot explain the ~100-fold shift in substrate affinity be-

Table 1. **Substrate transport properties of WT EAAT1 and R477H**

Substrate	Transporter	$K_{0.5}$			
		pH 5.5	pH 6.5	pH 7.5	pH 8.5
		µM	µM	µM	µM
L-glutamate	WT EAAT1	32 ± 3	25 ± 3	28 ± 6	41 ± 2
	R477H	0.70 ± 0.03	1.6 ± 0.2	9 ± 2	64 ± 8
L-aspartate	WT EAAT1	14 ± 2	19 ± 2	15 ± 3	33 ± 3
	R477H	2.0 ± 0.4	6.2 ± 0.4	13 ± 3	61 ± 3

L-Glutamate and L-aspartate concentration responses were measured in ND96 at pH 5.5, 6.5, 7.5, and 8.5 and fitted by least squares as a function of current at −60 mV to the Michaelis–Menten equation (Eq. 1) to obtain $K_{0.5}$ values for both glutamate and aspartate. Data shown represent the mean ± SEM ($n \geq 4$).

Downloaded from http://rupress.org/jgp/article-pdf/148/1/13/1795669/jgp_201511556.pdf by guest on 05 December 2025

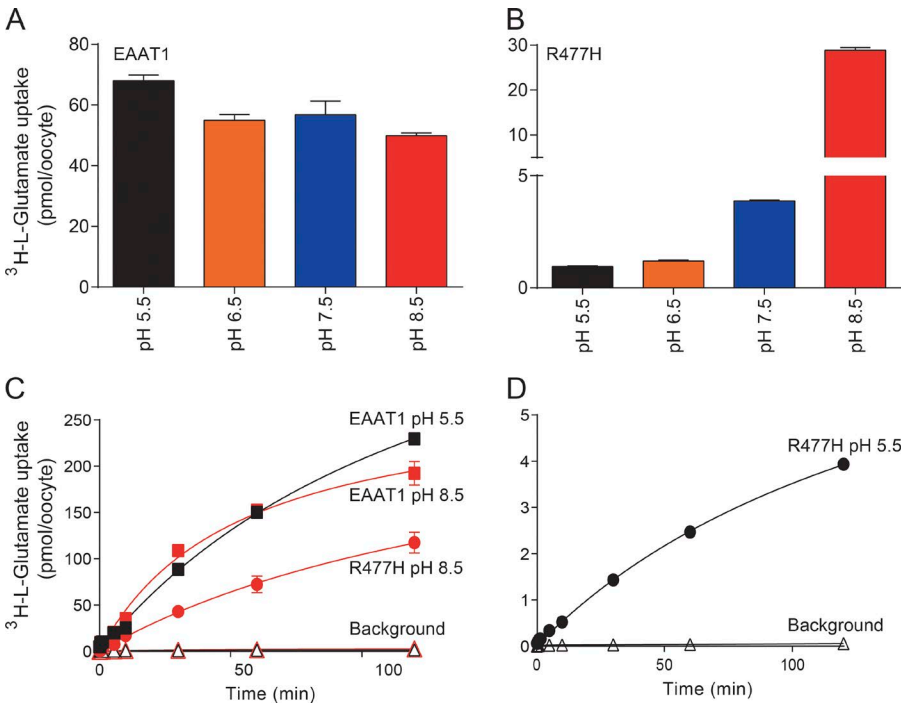

Figure 3. **R477H presents strong pH dependence for substrate transport.** Uptake of L-[^{3}H]glutamate into oocytes expressing WT EAAT1 (A) and R477H (B) was measured at pH 5.5 (black), 6.5 (orange), 7.5 (blue), and 8.5 (red) over a course of 10 min. Oocytes expressing WT EAAT1 were incubated in 10 µM L-[^{3}H]glutamate, and equivalent concentrations of L-[^{3}H]glutamate were used for oocytes expressing R477H to account for the shifts in $K_{0.5}$ for glutamate observed in this mutant transporter. See Materials and methods for further details. (C and D) Uptake of L-[^{3}H]glutamate, into oocytes expressing WT EAAT1 (squares) and R477H (circles), was measured over a 120-min time period at pH 8.5 (red) and pH 5.5 (black). 10 µM L-[^{3}H]glutamate was used for WT EAAT1 at both pH 5.5 and 8.5 and R477H at pH 8.5. 0.2 µM L-[^{3}H]glutamate was used for R477H at pH 5.5 to account for differences in substrate affinity. (D) Uptake for L-[^{3}H]glutamate into oocytes expressing R477H at pH 5.5 was lower than at pH 8.5 but is significantly above that of uninjected oocytes. A and B represent L-[^{3}H]glutamate of WT EAAT1– and R477H-expressing oocytes; background uptake is presented in C and D. Background refers to L-[^{3}H]glutamate uptake into uninjected oocytes for each condition. Data shown represent the mean ± SEM ($n \geq 7$). Where error bars cannot be seen, they lie within the symbol. Note the scale difference in the y axes.

tween WT EAAT1 and R477H observed at pH 5.5 (Fig. 4 B). In addition, the reversal potential of the TBOA-blocked leak conductance of R477H at pH 5.5 is not different to WT EAAT1 (Fig. 4 C), suggesting that the leak conductance remains selective for Cl^-. These data suggest that the integrity of the substrate and Na^+-binding sites are not affected by the R477H mutation and that the most likely explanation for the increased $K_{0.5}$ for glutamate is a slowing of the subsequent conformational changes associated with the elevator mechanism, resulting in a reduced turnover rate.

Cation versus anion permeation through R477H is pH dependent

To investigate whether a positively charged residue at position 477 determines anion selectivity of uncoupled EAAT1 conductances, current-voltage relationships for the R477H mutant transporter were determined at a range of pH values in both the absence and presence of permeant anions (Fig. 5). Under physiological conditions, glutamate application to oocytes expressing WT EAAT1 generates a current that is comprised of a coupled transport component and an uncoupled Cl^- component. The coupled transport component is inwardly directed at membrane potentials up to 60 mV; therefore, at positive membrane potentials (e.g., 60 mV), the outward current measured is because of the uncoupled Cl^- conductance (Fig. 5 A). When Cl^- in the recording buffer is exchanged for the impermeant anion gluconate, the application of glutamate to WT EAAT1 does not elicit an outward current at 60 mV as there are no available anions to permeate the uncoupled conductance pathway of the transporter (Fig. 5 B). In contrast, the application of glutamate to oocytes expressing the R477H mutant transporter activates outward currents at 60 mV in a gluconate-based buffer (Fig. 5 D). The amplitude of these currents increases as the pH of the recording buffer is increased to pH 8.5 in both Cl^- and gluconate-based buffers (Fig. 5, B and D). These results demonstrate that as the [H^+] decreases, and therefore the protonation of His-477 decreases, other ions are able to permeate the uncoupled conductance pathway. As there are no other anions in the recording solution, the conductance is likely to be carried by cations.

To investigate this further, we analyzed the effects of varying external [Na^+] on the reversal potential of glu-

Downloaded from http://rupress.org/jgp/article-pdf/148/1/13/1795669/jgp_201511556.pdf by guest on 05 December 2025

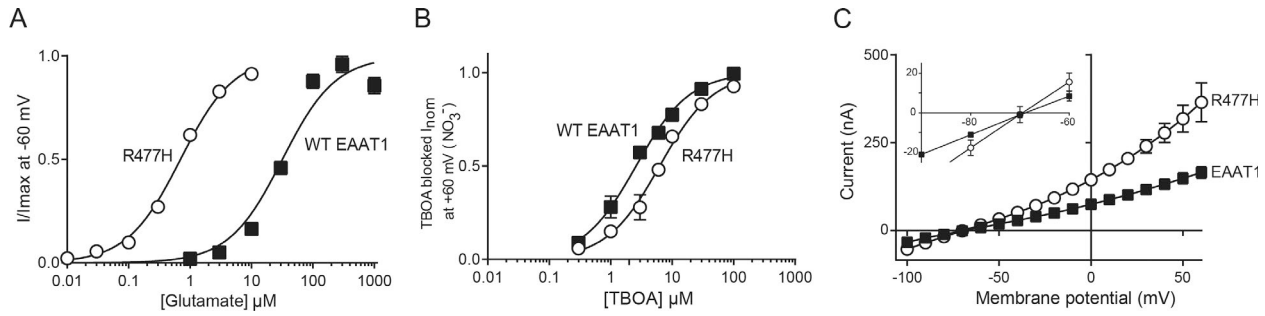

Figure 4. **The substrate-binding site is unperturbed in R477H at pH 5.5.** (A) Steady-state currents at 60 mV in the presence of increasing concentrations of the competitive blocker TBOA were measured in WT EAAT1 and the R477H mutant transporter at pH 5.5. These currents were then subtracted from currents in the absence of TBOA to measure the TBOA-dependent blockage of the Na^+-activated anion conductance. Currents were normalized to the maximal current blocked by TBOA for each cell. (B) L-Glutamate concentration responses for WT EAAT1 (closed squares) and R477H (open circles) at pH 5.5 reproduced from Fig. 2 are provided for comparison with [TBOA] concentration responses. (C) Current-voltage relationships for WT EAAT1 (closed squares) and R477H (open circles) as blocked by 30 μM TBOA at pH 5.5. Data shown represent the mean ± SEM ($n \geq 4$). Where error bars cannot be seen, they lie within the symbol.

tamate-activated conductances. Current-voltage relationships for WT EAAT1 and the R477H mutant transporter measured in 10 mM and 100 mM Na^+ reveal a decrease in current magnitude with decreasing external Na^+ (Fig. 6). This is caused by a decrease in the Na^+ driving force for substrate transport. Despite this reduction in transport, the reversal potentials measured for WT EAAT1 at both pH 5.5 and 8.5 and R477H at pH 5.5 were only slightly shifted with a 10-fold change in external Na^+ concentration (Fig. 6, A–C; and Table 2), which

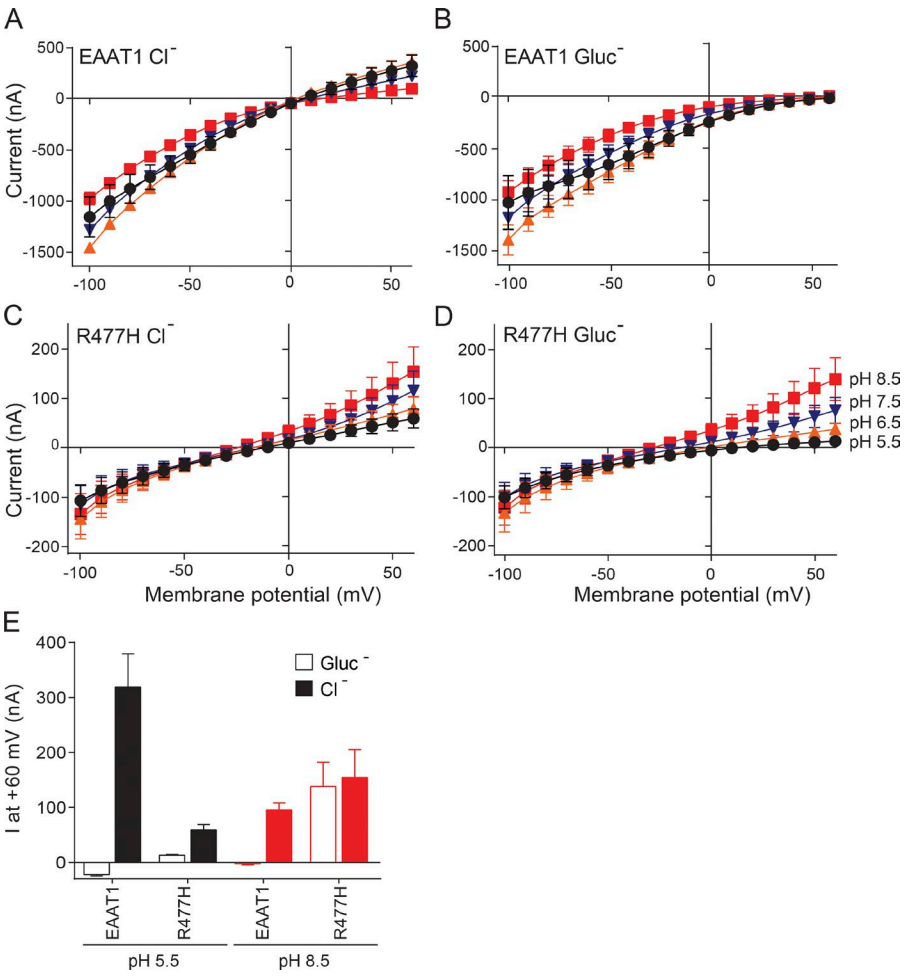

Figure 5. **pH-dependent uncoupled cation fluxes through R477H.** (A–D) Current-voltage relationships for WT EAAT1 and R477H elicited by submaximal L-glutamate in 96 mM Cl^--based buffer (A and C) and 96 mM gluconate-based buffer (B and D) at pH 5.5 (black circles), 6.5 (orange triangles), 7.5 (blue triangles), and 8.5 (red squares). (E) Current at 60 mV for WT EAAT1 and R477H at pH 5.5 (black) and 8.5 (red) in 96 mM gluconate-based buffer (open bars) and 96 mM Cl^--based buffer (closed bars). Data shown represent the mean ± SEM ($n \geq 4$). Where error bars cannot be seen, they lie within the symbol. Note the scale difference in the y axes.

Downloaded from http://rupress.org/jgp/article-pdf/148/1/13/1795669/jgp_201511556.pdf by guest on 05 December 2025

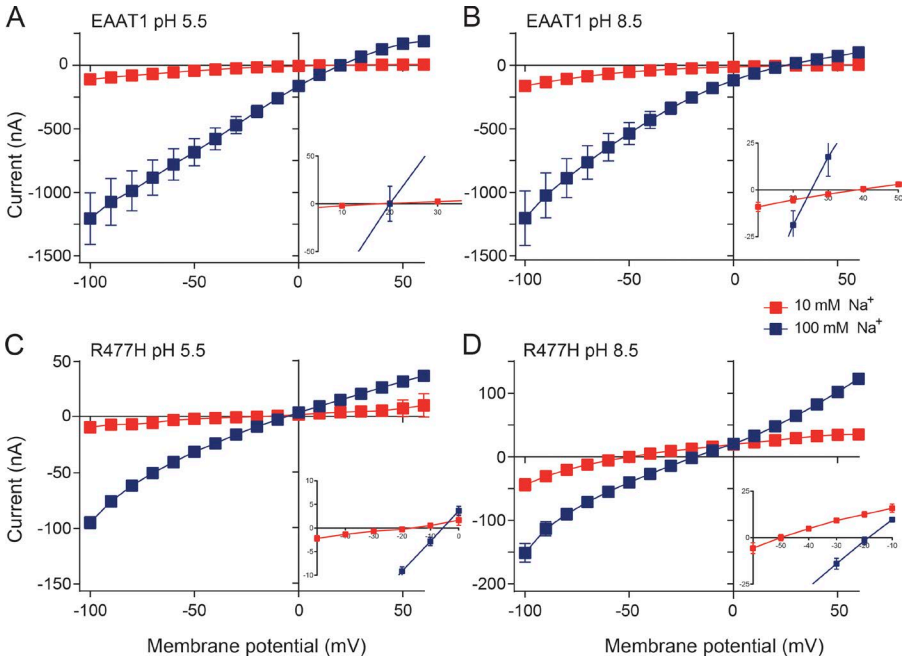

Figure 6. **Na^+ can permeate through R477H at pH 8.5.** (A–D) Current-voltage relationships for WT EAAT1 and R477H elicited by submaximal L-glutamate in 10 mM (red squares) and 100 mM (blue squares) Na^+-based buffers at pH 5.5 (A and C) and 8.5 (B and D). All buffers were osmotically balanced using choline$^+$ as the substitute cation. Data shown represent the mean ± SEM ($n \geq 4$). Where error bars cannot be seen, they lie within the symbol. Note the scale difference in the y axes.

suggests that Na^+ cannot permeate the uncoupled conductance pathway under these conditions. Conversely, current-voltage relationships for the R477H mutant transporter at pH 8.5 revealed a large negative shift in reversal potential from −19 ± 2 mV in 100 mM Na^+, to −52 ± 4 mV in 10 mM Na^+ (Fig. 6 D and Table 2), demonstrating that Na^+ ions can permeate the uncoupled conductance pathway of the R477H mutant transporter when His-477 is predominantly deprotonated.

Anions cannot permeate the uncoupled conductance pathway of R477H at pH 8.5

Although we have demonstrated that cations permeate the uncoupled conductance pathway of the R477H mutant transporter at pH 8.5, we were interested to see whether anions were still permitted entry into the channel under these conditions. When glutamate is applied to oocytes expressing EAAT1 in a Cl^--containing buffer, the magnitude of current at 60 mV is larger compared with that elicited when measured in the presence of the impermeant anion gluconate. This phenomenon was observed at both pH 5.5 and 8.5 as Cl^- is permeable through the uncoupled conductance pathway (Fig. 5 E). In the R477H mutant transporter, switching the external buffer from gluconate to Cl^- at pH 5.5 also resulted in an increase in current amplitude at 60 mV as His-477 is predominantly protonated and thus permits the permeation of Cl^- (Fig. 5 E). However, at pH 8.5, switching the external buffer from gluconate to Cl^- did not result in an increase in current at 60 mV (Fig. 5 E). This suggests that Cl^- ions are not able to permeate the mutant channel at pH 8.5 where His-477 is predominantly deprotonated. This observation was confirmed by measuring reversal potentials of the glutamate-elicited currents in 10 and 100 mM external Cl^- for both WT and R477H at pH 5.5 and 8.5 (Fig. 7 and Table 2). For WT EAAT1, this 10-fold decrease in external [Cl^-] at pH 5.5 and 8.5 resulted in a 34-mV and 18-mV positive shift in reversal potential, respectively, indicating that Cl^- can permeate the channel (Fig. 7, A and B; and Table 2). For glutamate-elicited currents in the R477H mutant transporter, a 27-mV positive shift in reversal potential with a 10-fold

Table 2. **Anion versus cation permeability through WT EAAT1 and R477H**

Ion	Concentration	E_{rev}			
		EAAT1		R477H	
		pH 5.5	pH 8.5	pH 5.5	pH 8.5
	mM	*mV*	*mV*	*mV*	*mV*
Na^+	10	18 ± 7	37 ± 4	−19 ± 3	−52 ± 4
	100	21 ± 4	26 ± 3	−6 ± 2	−19 ± 2
Cl^-	10	45 ± 3	52 ± 2	18 ± 3	−20 ± 3
	100	11 ± 2	34 ± 3	−9 ± 1	−18 ± 3

Reversal potential measurements (E_{rev}) for WT EAAT1 and R477H L-glutamate elicited currents at a range of Cl^- and Na^+ concentrations at pH 5.5 and 8.5. Choline-Cl^- and Na^+-gluconate were used to obtain correct osmotic balance. Data shown represent the mean ± SEM ($n \geq 4$).

Downloaded from http://rupress.org/jgp/article-pdf/148/1/13/1795669/jgp_201511556.pdf by guest on 05 December 2025

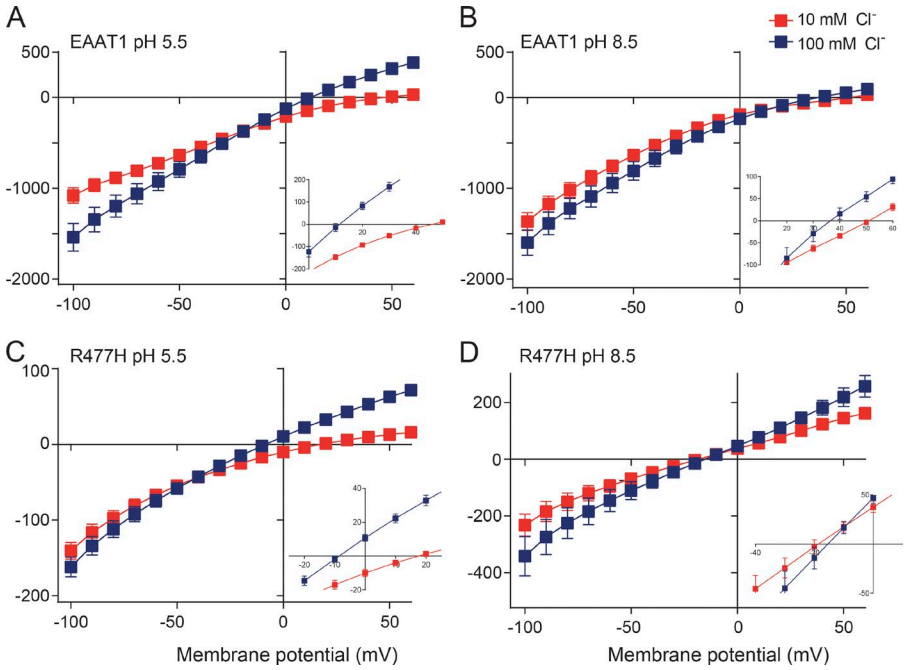

Figure 7. **Cl^- cannot permeate through R477H at pH 8.5.** (A–D) Current-voltage relationships for WT EAAT1 and R477H elicited by submaximal L-glutamate in 10 mM (red squares) and 100 mM (blue squares) Cl^--based buffers at pH 5.5 (A and C) and 8.5 (B and D). All buffers were osmotically balanced using gluconate$^-$ as the substitute anion. Data shown represent the mean ± SEM ($n \geq 4$). Where error bars cannot be seen, they lie within the symbol. Note the scale difference in the y axes.

change in external [Cl^-] was detected at pH 5.5 (Fig. 7 C). However, at pH 8.5, no such shift was observed (Fig. 7 D). This data further demonstrate that at pH 8.5, when His-477 is predominantly deprotonated, Cl^- is not able to permeate the uncoupled conductance pathway.

Although at pH 8.5 the R477H-uncoupled conductance pathway is selective for cations over Cl^-, we were interested to investigate whether the permeabilities of more permeant anions including Br^-, I^-, and NO_3^- through R477H were also pH dependent. At pH 5.5, significant changes in reversal potential measurements upon exchanging Cl^- for Br^-, I^-, and NO_3^- were observed for both WT EAAT1 and R477H (Table 3). These reversal potentials correspond to relative permeabilities (P_X^-/P_{Cl}^-) of 2.5 ± 0.1, 9.0 ± 0.5, and 11.1 ± 0.6 for WT EAAT1 and 1.75 ± 0.07, 5.8 ± 0.4, and 5.1 ± 0.5 for R477H, respectively (Table 3). Although the relative permeabilities are somewhat lower for the R477H mutant transporter, this transporter still demonstrates a significant preference for Br^-, I^-, and NO_3^- permeation over Cl^- permeation at pH 5.5.

It is not possible to measure relative anion permeabilities of the R477H transporter at pH 8.5 because Cl^- is not permeant. Complete substitution of Cl^- with Br^-, I^-, or NO_3^- at pH 8.5 did not result in any significant shifts in the reversal potentials of the glutamate activated currents (Table 3). However, in WT EAAT1 at pH 8.5, this anion substitution caused the reversal potential to shift from 50 ± 2 mV in Cl^-, to 46 ± 2, 16 ± 2, and 13 ± 2 mV in Br^-, I^-, and NO_3^-, respectively (Table 3). These results demonstrate that in addition to Cl^-, these alternate anions are also unable to permeate the uncoupled conductance pathway of the R477H mutant at pH 8.5. Thus, under conditions where R477H is likely to be predominantly deprotonated, the uncoupled conductance is truly cation selective. Together, these results support the hypothesis that a positive charge at position 477 is required for anion selectivity of the uncoupled conductance pathway. When this positive charge is removed, anions can no longer permeate this pathway, and the conductance switches to an uncoupled cation conductance.

Table 3. **Relative anion permeabilities of WT EAAT1 and R477H**

pH	Transporter	E_{rev}				P_X^-/P_{Cl}^-		
		Cl^-	Br^-	I^-	NO_3^-	P_{Br}^-/P_{Cl}^-	P_I^-/P_{Cl}^-	P_{NO3}^-/P_{Cl}^-
		mV	*mV*	*mV*	*mV*			
pH 5.5	EAAT1	51 ± 4	28 ± 3	−4 ± 3	−10 ± 3	2.5 ± 0.1	9.0 ± 0.5	11.1 ± 0.6
	R477H	14 ± 2	0 ± 1	−29 ± 1	−25 ± 2	1.75 ± 0.07	5.8 ± 0.4	5.1 ± 0.5
pH 8.5	EAAT1	50 ± 2	46 ± 2	17 ± 2	13 ± 2	1.19 ± 0.03	3.8 ± 0.2	4.4 ± 0.3
	R477H	−21 ± 3	−21 ± 3	−24 ± 3	−24 ± 2	ND	ND	ND

Reversal potentials (E_{rev}) of saturating L-glutamate–elicited currents were obtained in buffers containing 10 mM Cl^-, Br^-, I^-, and NO_3^- salts. Relative anion permeabilities were calculated from E_{rev} measurements using the Goldman–Hodgkin–Katz equation (Eq. 3). ND indicates that no relative anion permeability could be measured as Cl^- is not permeant through R477H at pH 8.5. Data shown represent the mean ± SEM ($n \geq 4$).

Downloaded from http://rupress.org/jgp/article-pdf/148/1/13/1795669/jgp_201511556.pdf by guest on 05 December 2025

DISCUSSION

In addition to transporting glutamate into cells, eukaryotic and prokaryotic members of the glutamate transporter family also contain Cl^- channel activity that plays a role in regulating cell excitability and osmotic balance (Veruki et al., 2006; Vandenberg et al., 2008, 2011). In this study, we have investigated the role of an arginine residue in regulating the dual functions of the human glutamate transporter, EAAT1. Arg-477 is in the transport domain of EAAT1 and is proximal to the substrate-binding site but is not predicted to directly interact with bound substrate (Boudker et al., 2007). Here, we have mutated this arginine residue to a histidine (R477H) and varied the pH of the recording buffer to demonstrate that a positive charge at position 477 is crucial for anion selectivity of the EAAT1-associated uncoupled conductance and that the nature of this residue also influences elevator movements of the transport domain involved in substrate transport.

The pK_a of free histidine in an aqueous environment is ∼6. We have exploited this property to finely tune the presence/absence of a positive charge at position 477 by manipulating the pH of our recording buffer. Using this approach, we are able to specifically examine the role of a positive charge at this position without changing other properties of the residue. At pH 5.5, where His-477 is predicted to be predominantly protonated, anion selectivity of the uncoupled conductance is preserved and is similar to WT EAAT1. In contrast, at pH 8.5, where the histidine is predicted to be mostly deprotonated, the uncoupled conductance is converted into a cation conductance. Remarkably, at pH 8.5 the conductance is a pure cation conductance, and anions are no longer able to permeate, suggesting that the positive charge at position 477 is not only required to prevent cation permeation, but also to actively attract anions. Furthermore, the effects of titrating R477H over this pH range on channel selectivity closely correlates with the pH titration of a free histidine, suggesting that this residue is located in an aqueous accessible environment in the pore of the channel.

The R477H mutant transporter also reveals a striking pH dependence of the $K_{0.5}$ for both glutamate and aspartate. At pH 5.5, the $K_{0.5}$ of the R477H mutant transporter for glutamate is ∼45-fold lower than that of WT EAAT1. As the $[H^+]$ of the recording buffer is decreased, this $K_{0.5}$ returned to one in the same range as WT EAAT1 at pH 8.5 (Fig. 2, D and E; and Table 1). When we measure the half-saturation of glutamate-activated transport currents ($K_{0.5}$), we are not directly measuring binding, but rather the whole ensemble of conformations that occur during substrate transport, including binding/unbinding and translocation. If any of these steps are affected by the mutation, a change in the $K_{0.5}$ will be observed. To examine which part of the transport cycle is affected by the R477H mutation, we used the nontransportable inhibitor TBOA, which can bind to the substrate-binding site but cannot be transported itself. Therefore, the $K_{0.5}$ measured for TBOA is equivalent to a measure of binding. Interestingly, the R477H mutation does not dramatically affect the ability of TBOA to bind (Fig. 4 A), suggesting that the substrate-binding site itself is not perturbed by the mutation. Therefore, we conclude that the large decrease in $K_{0.5}$ observed for R477H at pH 5.5 is likely caused by a slowing of the elevator movement during translocation, resulting in a reduced turnover rate. Indeed, the position of this arginine residue has been shown to be important in determining the turnover rate of both the EAATs and Glt_{Ph} (Ryan et al., 2010; Akyuz et al., 2015) and supports the notion that R477H does not affect the integrity of the binding site but rather the subsequent conformational changes required for transport. Additionally, the Na^+ $K_{0.5}$ value for R477H is minimally changed compared with WT EAAT1, indicating that the Na^+ dependence of transport is not affected by the R477H mutation at pH 5.5 (Fig. 2 F). Although it would be ideal to directly determine the stoichiometry of Na^+ coupling (Zerangue and Kavanaugh, 1996), these measurements need to be made in the absence of any uncoupled conductances. The effects of the R477H mutation prevent this type of analysis. At pH 8.5, the R477H mutation results in the activation of uncoupled cation conductances, which would interfere with the interpretation of reversal potential measurements required for determining Na^+ stoichiometry. At pH 5.5, the increase in substrate affinity and subsequent decrease in turnover rate result in currents that are too small to reliably measure in the absence of chloride.

We have shown that a positive charge at positon 477 in EAAT1 is required to select for anion permeation over cation permeation, but this residue does not appear to play a role in determining the selectivity between different permeant anions (Table 3). The selectivity sequence of the EAAT-associated anion conductance is of a lyotropic nature where larger anions are more permeant, indicating that removal of hydrating water molecules is the major barrier for entry of the anion into the channel. Consequently, electrostatic interactions with the anion selectivity filter are less important, and thus selectivity filters of anion channels with lyotropic selectivity typically feature polar residues rather than positively charged residues (Xu and Akabas, 1996; Smith et al., 1999; Hibbs and Gouaux, 2011). Indeed, polar residues at the domain interface of EAAT1 including Ser-103 and Thr-396 have been shown to be important in determining relative anion permeabilities (Ryan et al., 2004; Cater et al., 2014), whereas positively charged residues at the intracellular and extracellular vestibules of chloride channels are thought to attract anions into the channel. This is seen in the li-

Downloaded from http://rupress.org/jgp/article-pdf/148/1/13/1795669/jgp_201511556.pdf by guest on 05 December 2025

gand-gated anion channel family (Keramidas et al., 2004; Miller and Aricescu, 2014; Huang et al., 2015) and also in EAAT1 where residues located toward the extracellular edge of TM2 have been suggested to play a role in attracting anions into the channel (Ryan et al., 2004). We propose that Arg-477 may form a selectivity filter for anions over cations, and polar residues further along the pathway may provide further fine-tuning of anion selectivity and determine the relative permeabilities of the different anions.

In conclusion, we have demonstrated that the positive charge of Arg-477 is necessary for anion selectivity of the uncoupled conductance of EAAT1 and that the nature of this residue influences the elevator movement of the transport domain.

ACKNOWLEDGMENTS

We thank Cheryl Handford for her expert technical assistance and those who maintain the University of Sydney *Xenopus laevis* colony.

This work was supported by a National Health and Medical Research Council Project Grant (APP1048784). R.J. Cater is supported by an Australian Department of Education and Training Postgraduate Award and University of Sydney John Lamberton scholarship.

The authors declare no competing financial interests.

Merritt Maduke served as editor.

Submitted: 9 December 2015
Accepted: 17 May 2016

REFERENCES

Akyuz, N., E.R. Georgieva, Z. Zhou, S. Stolzenberg, M.A. Cuendet, G. Khelashvili, R.B. Altman, D.S. Terry, J.H. Freed, H. Weinstein, et al. 2015. Transport domain unlocking sets the uptake rate of an aspartate transporter. *Nature.* 518:68–73. http://dx.doi.org/10.1038/nature14158

Barish, M.E. 1983. A transient calcium-dependent chloride current in the immature *Xenopus* oocyte. *J. Physiol.* 342:309–325. http://dx.doi.org/10.1113/jphysiol.1983.sp014852

Borre, L., and B.I. Kanner. 2004. Arginine 445 controls the coupling between glutamate and cations in the neuronal transporter EAAC-1. *J. Biol. Chem.* 279:2513–2519. http://dx.doi.org/10.1074/jbc.M311446200

Borre, L., M.P. Kavanaugh, and B.I. Kanner. 2002. Dynamic equilibrium between coupled and uncoupled modes of a neuronal glutamate transporter. *J. Biol. Chem.* 277:13501–13507. http://dx.doi.org/10.1074/jbc.M110861200

Boudker, O., R.M. Ryan, D. Yernool, K. Shimamoto, and E. Gouaux. 2007. Coupling substrate and ion binding to extracellular gate of a sodium-dependent aspartate transporter. *Nature.* 445:387–393. http://dx.doi.org/10.1038/nature05455

Cater, R.J., R.J. Vandenberg, and R.M. Ryan. 2014. The domain interface of the human glutamate transporter EAAT1 mediates chloride permeation. *Biophys. J.* 107:621–629. http://dx.doi.org/10.1016/j.bpj.2014.05.046

Cater, R.J., R.M. Ryan, and R.J. Vandenberg. 2016. The split personality of glutamate transporters: A chloride channel and a transporter. *Neurochem. Res.* 41:593–599. http://dx.doi.org/10.1007/s11064-015-1699-6

Fairman, W.A., R.J. Vandenberg, J.L. Arriza, M.P. Kavanaugh, and S.G. Amara. 1995. An excitatory amino-acid transporter with properties of a ligand-gated chloride channel. *Nature.* 375:599–603. http://dx.doi.org/10.1038/375599a0

Grewer, C., P. Balani, C. Weidenfeller, T. Bartusel, Z. Tao, and T. Rauen. 2005. Individual subunits of the glutamate transporter EAAC1 homotrimer function independently of each other. *Biochemistry.* 44:11913–11923. http://dx.doi.org/10.1021/bi050987n

Hibbs, R.E., and E. Gouaux. 2011. Principles of activation and permeation in an anion-selective Cys-loop receptor. *Nature.* 474:54–60. http://dx.doi.org/10.1038/nature10139

Huang, X., H. Chen, K. Michelsen, S. Schneider, and P.L. Shaffer. 2015. Crystal structure of human glycine receptor-α3 bound to antagonist strychnine. *Nature.* 526:277–280. http://dx.doi.org/10.1038/nature14972

Keramidas, A., A.J. Moorhouse, P.R. Schofield, and P.H. Barry. 2004. Ligand-gated ion channels: mechanisms underlying ion selectivity. *Prog. Biophys. Mol. Biol.* 86:161–204. http://dx.doi.org/10.1016/j.pbiomolbio.2003.09.002

Koch, H.P., R.L. Brown, and H.P. Larsson. 2007. The glutamate-activated anion conductance in excitatory amino acid transporters is gated independently by the individual subunits. *J. Neurosci.* 27:2943–2947. http://dx.doi.org/10.1523/JNEUROSCI.0118-07.2007

Leary, G.P., E.F. Stone, D.C. Holley, and M.P. Kavanaugh. 2007. The glutamate and chloride permeation pathways are colocalized in individual neuronal glutamate transporter subunits. *J. Neurosci.* 27:2938–2942. http://dx.doi.org/10.1523/JNEUROSCI.4851-06.2007

Levy, L.M., O. Warr, and D. Attwell. 1998. Stoichiometry of the glial glutamate transporter GLT-1 expressed inducibly in a Chinese hamster ovary cell line selected for low endogenous Na^+-dependent glutamate uptake. *J. Neurosci.* 18:9620–9628.

Machtens, J.P., D. Kortzak, C. Lansche, A. Leinenweber, P. Kilian, B. Begemann, U. Zachariae, D. Ewers, B.L. de Groot, R. Briones, and C. Fahlke. 2015. Mechanisms of anion conduction by coupled glutamate transporters. *Cell.* 160:542–553. http://dx.doi.org/10.1016/j.cell.2014.12.035

Miller, P.S., and A.R. Aricescu. 2014. Crystal structure of a human GABAA receptor. *Nature.* 512:270–275. http://dx.doi.org/10.1038/nature13293

Owe, S.G., P. Marcaggi, and D. Attwell. 2006. The ionic stoichiometry of the GLAST glutamate transporter in salamander retinal glia. *J. Physiol.* 577:591–599. http://dx.doi.org/10.1113/jphysiol.2006.116830

Poulsen, M.V., and R.J. Vandenberg. 2001. Niflumic acid modulates uncoupled substrate-gated conductances in the human glutamate transporter EAAT4. *J. Physiol.* 534:159–167. http://dx.doi.org/10.1111/j.1469-7793.2001.00159.x

Reyes, N., C. Ginter, and O. Boudker. 2009. Transport mechanism of a bacterial homologue of glutamate transporters. *Nature.* 462:880–885. http://dx.doi.org/10.1038/nature08616

Ryan, R.M., and J.A. Mindell. 2007. The uncoupled chloride conductance of a bacterial glutamate transporter homolog. *Nat. Struct. Mol. Biol.* 14:365–371. http://dx.doi.org/10.1038/nsmb1230

Ryan, R.M., and R.J. Vandenberg. 2002. Distinct conformational states mediate the transport and anion channel properties of the glutamate transporter EAAT-1. *J. Biol. Chem.* 277:13494–13500. http://dx.doi.org/10.1074/jbc.M109970200

Ryan, R.M., and R.J. Vandenberg. 2005. A channel in a transporter. *Clin. Exp. Pharmacol. Physiol.* 32:1–6. http://dx.doi.org/10.1111/j.1440-1681.2005.04164.x

Ryan, R.M., and R.J. Vandenberg. 2016. Elevating the alternating-access model. *Nat. Struct. Mol. Biol.* 23:187–189. http://dx.doi.org/10.1038/nsmb.3179

Downloaded from http://rupress.org/jgp/article-pdf/148/1/13/1795669/jgp_201511556.pdf by guest on 05 December 2025

Ryan, R.M., A.D. Mitrovic, and R.J. Vandenberg. 2004. The chloride permeation pathway of a glutamate transporter and its proximity to the glutamate translocation pathway. *J. Biol. Chem.* 279:20742–20751. http://dx.doi.org/10.1074/jbc.M304433200

Ryan, R.M., E.L. Compton, and J.A. Mindell. 2009. Functional characterization of a Na^+-dependent aspartate transporter from *Pyrococcus horikoshii*. *J. Biol. Chem.* 284:17540–17548. http://dx.doi.org/10.1074/jbc.M109.005926

Ryan, R.M., N.C. Kortt, T. Sirivanta, and R.J. Vandenberg. 2010. The position of an arginine residue influences substrate affinity and K^+ coupling in the human glutamate transporter, EAAT1. *J. Neurochem.* 114:565–575. http://dx.doi.org/10.1111/j.1471-4159.2010.06796.x

Seal, R.P., Y. Shigeri, S. Eliasof, B.H. Leighton, and S.G. Amara. 2001. Sulfhydryl modification of V449C in the glutamate transporter EAAT1 abolishes substrate transport but not the substrate-gated anion conductance. *Proc. Natl. Acad. Sci. USA.* 98:15324–15329. http://dx.doi.org/10.1073/pnas.011400198

Smith, S.S., E.D. Steinle, M.E. Meyerhoff, and D.C. Dawson. 1999. Cystic fibrosis transmembrane conductance regulator. Physical basis for lyotropic anion selectivity patterns. *J. Gen. Physiol.* 114:799–818. http://dx.doi.org/10.1085/jgp.114.6.799

Torres-Salazar, D., J. Jiang, C.B. Divito, J. Garcia-Olivares, and S.G. Amara. 2015. A mutation in transmembrane domain 7 (TM7) of excitatory amino acid transporters disrupts the substrate-dependent gating of the intrinsic anion conductance and drives the channel into a constitutively open state. *J. Biol. Chem.* 290:22977–22990. http://dx.doi.org/10.1074/jbc.M115.660860

Vandenberg, R.J., and R.M. Ryan. 2013. Mechanisms of glutamate transport. *Physiol. Rev.* 93:1621–1657. http://dx.doi.org/10.1152/physrev.00007.2013

Vandenberg, R.J., S. Huang, and R.M. Ryan. 2008. Slips, leaks and channels in glutamate transporters. *Channels (Austin).* 2:51–58. http://dx.doi.org/10.4161/chan.2.1.6047

Vandenberg, R.J., C.A. Handford, E.M. Campbell, R.M. Ryan, and A.J. Yool. 2011. Water and urea permeation pathways of the human excitatory amino acid transporter EAAT1. *Biochem. J.* 439:333–340. http://dx.doi.org/10.1042/BJ20110905

Verdon, G., and O. Boudker. 2012. Crystal structure of an asymmetric trimer of a bacterial glutamate transporter homolog. *Nat. Struct. Mol. Biol.* 19:355–357. http://dx.doi.org/10.1038/nsmb.2233

Veruki, M.L., S.H. Mørkve, and E. Hartveit. 2006. Activation of a presynaptic glutamate transporter regulates synaptic transmission through electrical signaling. *Nat. Neurosci.* 9:1388–1396. http://dx.doi.org/10.1038/nn1793

Wadiche, J.I., and M.P. Kavanaugh. 1998. Macroscopic and microscopic properties of a cloned glutamate transporter/chloride channel. *J. Neurosci.* 18:7650–7661.

Wadiche, J.I., S.G. Amara, and M.P. Kavanaugh. 1995. Ion fluxes associated with excitatory amino acid transport. *Neuron.* 15:721–728. http://dx.doi.org/10.1016/0896-6273(95)90159-0

Xu, M., and M.H. Akabas. 1996. Identification of channel-lining residues in the M2 membrane-spanning segment of the GABA(A) receptor alpha1 subunit. *J. Gen. Physiol.* 107:195–205. http://dx.doi.org/10.1085/jgp.107.2.195

Yernool, D., O. Boudker, Y. Jin, and E. Gouaux. 2004. Structure of a glutamate transporter homologue from *Pyrococcus horikoshii*. *Nature.* 431:811–818. http://dx.doi.org/10.1038/nature03018

Zerangue, N., and M.P. Kavanaugh. 1996. Flux coupling in a neuronal glutamate transporter. *Nature.* 383:634–637. http://dx.doi.org/10.1038/383634a0

Downloaded from http://rupress.org/jgp/article-pdf/148/1/13/1795669/jgp_201511556.pdf by guest on 05 December 2025